Molecular Modeling of Interactions between L-Lysine and a Hydroxylated Quartz Surface

G. Laura Gambino,[†] Giuseppe M. Lombardo,[‡] Antonio Grassi,[‡] and Giovanni Marletta*[,†]

Dipartimento di Scienze Chimiche, Via Andrea Doria 6, Facoltà di Scienze MM.FF.NN., University of Catania, I-95125 Catania, Italy, and Dipartimento di Scienze Chimiche, Via Andrea Doria 6, Facoltà di Farmacia, University of Catania, I-95125 Catania, Italy

Received: July 10, 2003; In Final Form: October 15, 2003

The static and dynamical properties of L-lysine adsorbed onto a hydroxylated quartz surface were modeled by using semiempirical quantum mechanics and force field techniques. Both semiempirical and force field calculations indicate that a strong interaction occurs between the ϵ-protonated amino group of L-lysine with the surface. Furthermore, the amino acid molecule has a preferred end-on orientation, with the ϵ-protonated amino group pointing toward the surface. The statistical analysis of the system trajectories reveals that the relatively ordered water-shell structure of the amino acid molecule in the "bulk" solution is broken when the molecule approaches the surface because of the reciprocal perturbation of the molecule and surface solvation shells.

1. Introduction

There is growing interest in the understanding of the interaction and anchoring process of simple amino acids and oligopeptides onto solid surfaces, in view of their applications in different areas such as biotechnology, biomaterials, biosensors, bioseparation, and so forth.[1]

Despite the relatively small size of these molecules, the detailed mechanism of their interaction with solid surfaces is not yet properly understood because of the complexity of the system formed by the biomolecule and its environment. Among the many relevant open issues, critically determining the interaction of an amino acid or oligopeptide with a solid surface, the problem of the solvent and particularly of water play key roles[2] because of the fact that the biomolecule adsorption process is considered in some way to occur through its trapping by the network of water molecules on the surface.

Regarding the static properties of amino acids in solution, theoretical ab initio studies have been published on L-glycine,[3,4] L-α-alanine,[5] L-valine,[6] and L-serine,[7] and molecular dynamics (MD) studies have been focused on the structural change of water around the amino acid and its general dynamical properties.[8]

However, a huge amount of experimental and theoretical effort has been performed to clarify the water structure on different solid surfaces. Among solid surfaces, silica-based surfaces and especially quartz are particularly interesting because of their applications as model surfaces in several biological and technological problems.[9] The interaction of quartz surfaces with water has been extensively characterized by using measurements of ζ-potential,[10] dissolution kinetics,[11,12] and IR observations of surface groups[13] as well as by using ab initio calculations[14,15] and molecular dynamic[16] aimed at extracting a rigorous picture of the SiO_2/H_2O interface and the charging behavior of SiO_2 in aqueous solution.[17] Finally, West et al. have studied L-lysine[18] and L-alanine[19] interactions with silica clusters under vacuum conditions by means semiempirical calculations.

L-Lysine [(2*S*)-2,6-diamminocapronic acid, $NH_2(CH_2)_4CH(NH_2)COOH$] is an essential amino acid characterized by an amine group at the ϵ-C position. Its side chain has a relevant biological role in, for example, its control of the adsorption of plasminogen,[20] the albumin interaction with drugs,[21] and GHK properties.[22]

The present paper reports the theoretical results obtained by using quantum mechanic, molecular mechanic, and molecular dynamic codes to simulate the adsorption process of L-lysine onto hydroxylated quartz at the isoelectric pH (9.5) of the amino acid. Specific attention has been paid to the clarification of the structure of the interfacial region, where the interaction between hydrated atoms of the surface and the hydrated amino acid molecule is localized.

2. Methods

Computational Methods. Quantum mechanics calculations were performed at the Hartree−Fock level (HF) using semiempirical Hamiltonian AM1 included in the MOPAC 2000 program.[23] In fact, the AM1 code is specially parametrized for silicon, oxygen, and hydrogen as well as for carbon and nitrogen and the chemical reactions between molecules containing these elements.

The solvent effect was taken into account by using both the conductor screening model (COSMO)[24] and by introducing explicit water molecules. In fact, in the COSMO technique the solute molecule is embedded in a dielectric continuum of permittivity ϵ that represents the solvent. The parameters used for these calculations were 60 segments per atom and $\epsilon = 78.4$ (as for water). All structures were optimized to a gradient norm of 0.01 using the eigenvector following method (EF). The results of MOPAC calculations are reported in terms of the heat of formation, defined as the sum of the electronic energy E_e, the nuclear−nuclear repulsion energy E_n, the energy E_{isol} required to strip off all valence electrons of the atoms in the system, and the total heat of atomization E_{atom} of all atoms in the system:

$$\Delta H_f = E_e + E_n + \sum E_{isol} + \sum E_{atom} \qquad (1)$$

* Corresponding author. E-mail: marletta@dipchi.unict.it.
[†] Facoltà di Scienze MM.FF.NN., University of Catania.
[‡] Facoltà di Farmacia, University of Catania.

10.1021/jp035991s CCC: $27.50
Published on Web 01/31/2004

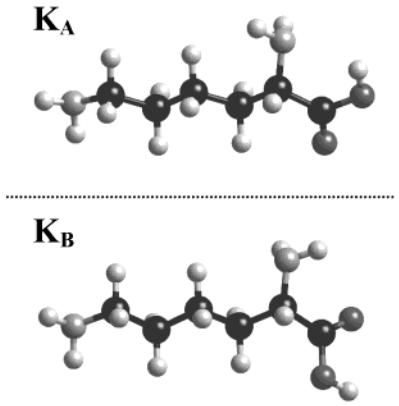

Figure 1. Optimized structures of neutral conformers (K_A and K_B) of L-lysine in the gas phase.

SCHEME 1: Equilibrium Representation of Three Principal Form of Lysine−K1, K2, and K3−at the Isoelectric pH

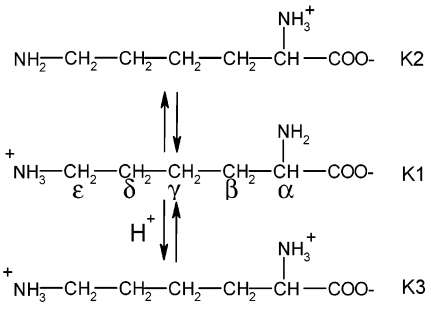

The MD simulations were performed with the TINKER 4.0 code[25] using the MM3(2000)[26a,b] force field (MM3-FF) and periodic boundary conditions (PBC) with the minimum image convention. The parametrization of MM3-FF was obtained from ab initio calculations, fitted to experimental data.[26c,d] The dielectric constant was set equal to 1, and the cutoff distance for nonbonding interactions was set equal to 12.5 Å. All MD simulations were performed under NVT conditions (volume and temperature) at 298 K with a 1-fs time step. After initial geometry optimization, the system was equilibrated for 40 ps and then was allowed to run for 60 ps.

Structural Model. The initial structures of L-lysine[27] and the silica surface[28] were obtained from the experimental data. At room temperature, L-lysine is a white crystalline solid that exists in the zwitterionic form $NH_3^+(CH_2)_4CH-(NH_2)COO^-$. In aqueous solution, the L-lysine form depends on the pH value, varying from the divalent cationic form $NH_3^+(CH_2)_4CH-(NH_3^+)COOH$ to the monovalent cationic form $NH_3^+(CH_2)_4-CH-(NH_3^+)COO^-$ to the zwitterionic form $NH_3^+(CH_2)_4CH-(NH_2)COO^-$ on anionic $NH_2(CH_2)_4CH-(NH_2)COO^-$ as pH increases.

The pK_a values for the three last forms are 2.2, 9.1, and 10.7,[29] respectively. We have studied the three dominant forms of L-lysine present at the isoelectric pH (9.5): the zwitterionic forms, with the ϵ-amino group protonated (indicated as K1) or with the α-amino group protonated (indicated as K2), and the positively charged form, with both amino groups protonated (indicated as K3) (Scheme 1).

We have also considered the two most stable neutral conformers in the gas phase, indicated in Figure 1 as K_A and K_B.

In the starting amino acid structure, the values of dihedral angles are set equal to 180° so that the side-chain conformations are extended. The MD simulation of L-lysine is carried out by soaking the amino acid into a cubic box of 24.66 Å with 500 water molecules.

The initial structure of the silica cluster is built from an α-quartz unit cell by replicating it $3 \times 3 \times 2$ along the *a*, *b*, and *c* directions. Cleaving this supercell along the (001) plane between two oxygen layers, the oxygen atoms in the bottom layer were saturated with hydrogen. The atoms of the last layer are kept fixed during the geometry optimization. This preliminary optimization showed that a reconstruction of the first layer occurs under vacuum conditions involving the oxygen atoms, which relax with respect to their bulk position, decreasing the Si−O bond length from 1.64 to 1.53 Å while Si−O−Si bond angle becomes 126.0°, deviating considerably from the tetrahedral value. Consequently, the terminal SiO_3 group is nearly planar, in agreement with recent literature.[14] After introducing into the system six water molecules and after geometry optimization in the UHF scheme, we found that the formation of geminal silanols occurred. Starting from this optimized structure, we have saturated the dangling bonds with OH groups, building a cluster of $H_{60}Si_{42}O_{114}$.

In the successive step, a negative charge was introduced on the silica surface by means of the deprotonations of the silanolic groups in order to obtain a surface charge density of 0.21 *e* nm^{-2}, corresponding to what is expected at the isoelectric point for L-lysine at pH 9, in agreement with the value measured by using the ζ-potential technique.[29]

The reliability of the AM1 method with respect to this step has been tested by calculating the gas-phase acidity of H_4SiO_4 (i.e., for the reaction $H_4SiO_{4(g)} \rightarrow [H3SiO_4]^-_{(g)} + H^+_{(g)}$). The calculation, after correcting the result for the $\Delta H_{form}(H^+)$, provided a value of ΔH_{reac} of 360.00, in nice agreement with the value reported for ab initio calculations performed by using 6-311+G**//3-21G** (361.00 kcal/mol) or MP2/6-31G* with a 3-21G** ZPE correction (374.00 kcal/mol).[30]

Globally, the system studied at the static level by using semiempirical calculations contains the optimized silica cluster ($H_{56}Si_{42}O_{114}$), 1 L-lysine, and 10 water molecules, as reported in Figure 2a.

At variance with this, for MD simulations we have built a silica slab of $25.5 \times 24.9 \times 8.21$ placed in a box with a *c* axis of 60 Å and with 350 water molecules and by using periodic boundary conditions (PBC), as shown in Figure 2b. To run the calculations, we have chosen three starting configurations for the molecular arrangement between the silica surface and L-lysine.

The three configurations correspond to the three following orientations of the amino acid with respect to the surface: an end-on configuration, either with the backbone of the molecule perpendicular to the surface and the ϵ-amino group toward to the surface (a) or with the α-amino group oriented toward the surface (b); a side-on configuration, with the backbone parallel to the surface (c). The resulting configuration for each form (K1, K2, and K3 described above) will be henceforth indicated as K*xy*, with $x = 1, 2, 3$ and $y = a, b, c$.

3. Results

3.1. Solvation Effects on L-Lysine: Static and Dynamic Simulations. The structure determination of biomolecules in the gas phase is not a simple problem. These molecules can exhibit several conformations, many of which are isoenergetic. However, in the liquid phase, because of solvent stabilization, the number of conformations decreases considerably, and in case of amino acids, the zwitterionic configuration is the main

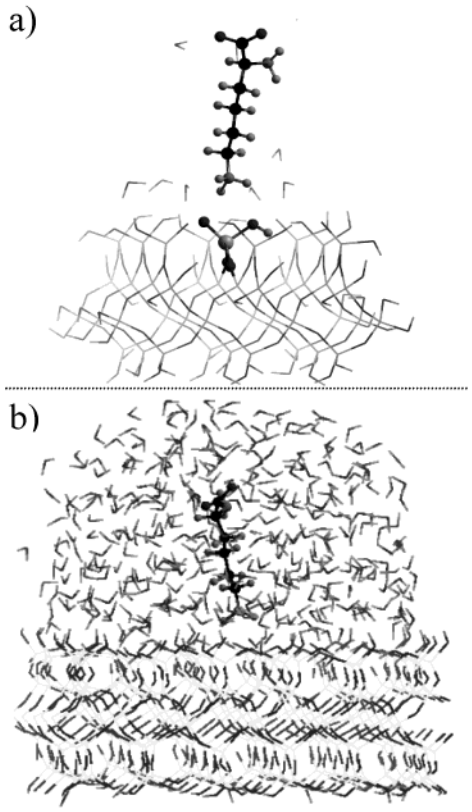

Figure 2. Simulated systems: (a) in semiempirical calculations (formed by the silica cluster (H56Si42O114), 1 L-lysine, and 10 water molecules); (b) in MD simulations (formed by a silica slab of 25.5 × 24.9 × 8.21 placed in a box with a *c* axis of 60 Å and with 350 water molecules and 1 L-lysine).

TABLE 1: Enthalpy of Formation (ΔH_f) (kcal/mol) of the Different Forms of L-Lysine[a]

ΔH_f (kcal/mol)	gas	COSMO	ΔH_{solv}
K_A	−115.5	−143.3	−27.8
K_B	−121.1	−146.9	−25.8
K1	−36.14	−166.0	−129.9
K2	−83.2	−161.0	−77.8
K3	39.8	−82.1	−121.9

[a] Neutral (KA and KB), zwitterionic (K1 and K2), and charged (K3) in the gas phase and in solution (COSMO). The enthalpy of solvation is calculated as $\Delta H_{COSMO} - \Delta H_{gas}$.

structure. In water, amino acids tend to assume a linear conformation due to dipole−dipole interactions of the carboxylic and amino groups with the water molecules. We have focused our attention on the species present in solution at the isoelectric pH value at which we have performed experimental measurements reported in a related paper.[31]

In Table 1, the enthalpy variation ΔH_f for two neutrals (K_A, K_B), zwitterionic (K1 and K2), and cationic (K3) forms in gas and in solution (obtained by the COSMO technique) are reported.

In the gas phase, the most stable configurations are the neutral forms and in particular K_B. This structure is about 40 kcal/mol more stable with respect to the zwitterionic structures, which in any case are not very meaningful in the gas phase. Note that the K_A form displays a cyclelike conformation where the carboxylic and the amino groups form intramolecular hydrogen bonds between the −OH of the carboxyl group and the nitrogen atom of the amino group in the α position, respectively. At variance with this, in the K_B form the carboxylic group is rotated

TABLE 2: Calculated Enthalpic and Entropic Contributions to the Variation of Free Energy for the K1 and K2 Forms[a]

	K1		K2	
	gas	solution	gas	solution
ΔH	8.16	8.62	8.13	8.55
ΔS	0.11	0.86	0.11	0.633
ΔG	−25.74	−104.3	−25.44	−103.1

[a] Values are in kcal/mol. The solution is simulated by introducing explicit water molecules.

180° around the C−C bond, prompting the formation of an intramolecular hydrogen bond between the carbonylic oxygen and the hydrogen of the amino group in the α position (Figure 1). In solution, the zwitterionic structures are more stable than the K_A and K_B forms because of the fact that the solvation energy, calculated as $\Delta H_{solv} = \Delta H_{COSMO} - \Delta H_{gas}$, increases on going from K_A to K1. These results are easily explained in terms of the magnitude of the calculated gas-phase dipole moments ($\mu_{K_A} = 4.55$ D, $\mu_{K_B} = 3.98$ D, $\mu_{K1} = 32.82$ D, $\mu_{K2} = 10.55$ D). Indeed, it is well known that dipolar solvents such as water better stabilize molecules (or molecular configurations) with higher dipole moment, such as K1 in the present case. Furthermore, the greater stability of K1 in solution is also related to the fact that the terminal ϵ-amino group is more basic than the α-amino group.

The solvation effect also has a specific structural aspect involving the fact that in solution the H-bonds' length between COO^- and the hydrogen in the amino group in α increases with respect to that in the gas form because of the screening effect induced by the solvent. It is noteworthy that this feature is present in both the employed strategies for calculating the solvation effect (i.e., COSMO) and in explicit calculations including the water molecules.

On the basis of the calculated total energy of the system, we could derive a value of 0.78 for the constant of K1 ⇔ K2 equilibrium on the basis of the result that $\Delta G^0 \approx \Delta H^0$, as far as the calculated entropic contribution is approximately the same for the two K1 and K2 species (Table 2).

The positively charged form of L-lysine, K3, shows the highest energy in the gas phase with a distorted conformation that does not occur in solution, where the linear conformation is preferred.

We have also performed several simulations to include explicitly the contribution of water molecules by considering a periodic box containing a molecule of L-lysine with different numbers of water molecules. We stress the fact that it resulted from several test calculations (not reported here) that a relatively high number of water molecules is needed to simulate correctly the solvation energy. In particular, a suitable simulation was achieved by using 10 water molecules.

The simulations show that for both the zwitterionic and the protonated forms the amino acid molecule still maintains a nonlinear conformation when there are up to 10 water molecules, whereas the most stable conformation in bulk solution, simulated by including in the calculation more than 10 water molecules, is linear. This result perfectly coincides with the results of a simulation accounting for the medium by an average dielectric constant, as in the COSMO calculation.

Molecular dynamic simulations of the three forms of L-lysine (K1, K2, and K3), explicitly including water molecules, allow us to evaluate the properties of the solution environment in terms of the formation of hydration shells. Accordingly, the analysis of MD trajectories was performed by following the time evolution of the dihedral angles and also the radial distribution

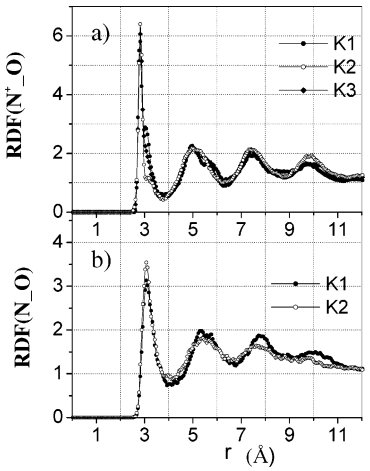

Figure 3. Radial distribution functions for L-lysine in MD simulations in a water box: (a) RDF of water oxygen around the L-lysine nitrogen of ammonium group atoms (N^+) for the K1, K2, and K3 forms; (b) RDF of water oxygen around the L-lysine nitrogen of amine group atoms (N) for the K1 and K2 forms.

TABLE 3: Time-Averaged ⟨Φ⟩ and Standard Deviation σ of Backbone Dihedral Angles Reported for the Three Forms K1, K2, and K3

	K1		K2		K3	
Φ	⟨Φ⟩	σ	⟨Φ⟩	σ	⟨Φ⟩	σ
$N_\epsilon-C_\epsilon-C_\delta-C_\gamma$	180.37	10.40	177.17	11.03	188.48	10.26
$C_\epsilon-C_\delta-C_\gamma-C_\beta$	176.35	11.40	178.56	10.98	287.40	11.62
$C_\delta-C_\gamma-C_\beta-C_\alpha$	178.25	8.93	169.88	7.80	182.40	6.96
$C_\gamma-C_\beta-C_\alpha-N_\alpha$	187.47	10.73	279.75	10.97	171.13	9.93

functions of the water molecules around the nitrogen and oxygen atoms of the amino acid.

The time-dependent calculations of the relevant dihedral angles performed for the K1−K3 forms showed only small fluctuations around their equilibrium values, indicating that the backbones have restricted movements, practically corresponding to a rigid conformation (Table 3).

The hydration properties were studied by analyzing the radial distribution functions (RDF) of water around N_α, N_ϵ, C_1, and O_k (Scheme 1). Figure 3 reports the RDF profiles of the oxygen atoms of water around the ammonium group and the amine group. The curves show very sharp polar features diagnostic of well-structured hydration shells.

The radial distribution function RDF(N^+−O) shows the first peak at 2.8 Å, and the RDF(N−O) shows the first peak at 3.1 Å, being half the height of the former one, thus indicating that N^+ is more hydrated than N.

3.2. L-Lysine−Surface Interactions: Static and Dynamic Simulations. To understand the orientational effect of the molecule−surface interactions, we have calculated the interaction energy (ΔH_i) between L-lysine and the silica surface for different molecular orientations by means of the semiempirical AM1 method.

Preliminarily, to test the reliability of the AM1 semiempirical methods and of the MM3 force field, we compared the bond angles and distances respectively for the quartz crystal (Table 4) and the K1 structure calculated in the gas phase (Table 5) with the relevant experimental data. The simulation for quartz was performed for both methods by fixing all of the cell parameters.

Furthermore, we have also calculated the L-lysine−O−Si hydrogen bonding energy for the K1, K2, and K3 geometries reported in Figure 4 by using both AM1 and MM3. The results

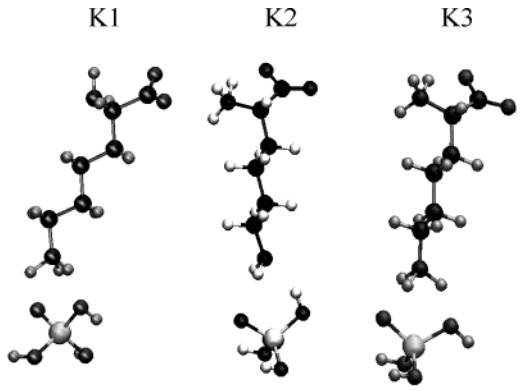

Figure 4. Fixed geometry for K1, K2, and K3 used to evaluate the H-bond energy by using AM1 and MM3 calculations.

TABLE 4: Comparison of the Bond Lengths (Å) and Bond Angles (deg) in Quartz Optimized within AM1 and MM3 and Those Obtained from Experimental Data

	AM1	MM3	exptl[28]
Si−O	1.72	1.63	1.63
SiO−H	0.95	0.96	0.95
SiOSi	143	141.2	143.1
OSiO	109.5	110.4	109.5
SiOH	114.2	119.7	119.5

TABLE 5: Comparison of the Bond Lengths (Å) and Dihedral Angles (deg) in L-Lysine Optimized within AM1 and MM3 and Those Obtained from Experimental Data

	AM1	MM3	exptl[27]
C_1-O_k	1.2591	1.2757	1.25
$C_\alpha-N_\alpha$	1.4565	1.4568	1.48
$C_\epsilon-N_\epsilon$	1.4980	1.5014	1.51
$C_\gamma-C_\beta-C_\alpha-N_\alpha$	−65.25	−63.23	−56.4
$C_\delta-C_\gamma-C_\beta-C_\alpha$	−176.12	−179.67	−176.0
$C_\epsilon-C_\delta-C_\gamma-C_\beta$	−175.80	−178.90	−171.1
$N_\epsilon-C_\epsilon-C_\delta-C_\gamma$	177.28	178.18	179.2

TABLE 6: Enthalpy of Formation (ΔH_f) (kcal/mol) of the Simulated Systems and Interaction Energy (ΔH_i) between L-Lysine and the Silica Surface for Different Molecular Orientations Obtained from AM1 Calculations[a]

	ΔH_f (kcal/mol)	ΔH_i (kcal/mol)
c-K1a	−9941.0	−20.92
c-K1b	−9970.3	−50.16
c-K1c	−9980.0	−59.86
c-K2a	−9964.8	−24.02
c-K2b	−9985.1	−44.34
c-K2c	−9953.4	−12.67
c-K3a	−10045.0	−151.50
c-K3b	−10062.3	−168.77
c-K3c	−10018.4	−124.92

[a] $\Delta H_i = \Delta H_{f(tot)} - \Delta H_{f(lys)} - \Delta H_{f(c-SiO_2+10H_2O)} - \Delta H_{solv(lys)}$, where $\Delta H_{f(lys)}$ is relative to lysine in gas phase, $\Delta H_{f(c-SiO_2+10H_2O)}$ is relative to the surface with ten water molecules, and $\Delta H_{solv(lys)}$ is the solvation enthalpy of lysine.

show that the difference in energy found with the two methods is only 1.41 kcal/mol for K1, 3.26 kcal/mol for K2, and 4.01 kcal/mol for K3 forms, indicating that the MM3 results are at this level quite reliable when compared with the AM1 method.

In particular, Table 6 reports the total $\Delta H_{f(tot)}$ of the system and ΔH_i. ΔH_i was estimated according to the following equation:

$$\Delta H_i = \Delta H_{f(tot)} - \Delta H_{f(lys)} - \Delta H_{f(c-SiO_2+10H_2O)} - \Delta H_{solv(lys)} \quad (2)$$

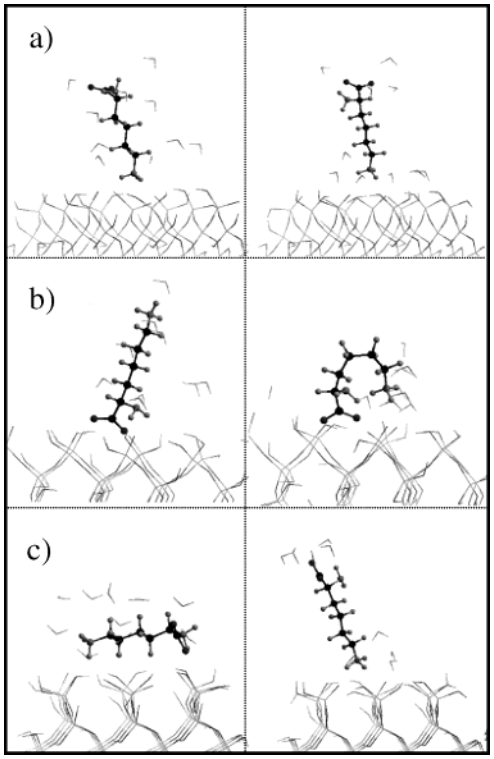

Figure 5. AM1 initial (left column) and optimized (right column) geometries of L-lysine in the K1 form in the three orientation: (a) end-on, with the ϵ-amino group pointing toward the surface, (b) end-on with the α-amino group pointing toward the surface, and (c) side-on.

where $\Delta H_{f(lys)}$ is relative to L-lysine in the gas phase, $\Delta H_{f(c-SiO_2+10H_2O)}$ is relative to the surface with 10 water molecules, and $\Delta H_{solv(lys)}$ is the solvation enthalpy of L-lysine.

In Figure 5, the starting (left) and optimized (right) structures for K1 are reported. The final optimized structures for K1a and K1c show the same orientation, and K1b presents a bent structure with both nitrogen atoms oriented toward the surface. ΔH_i (Table 6) for K1c is the lowest among the three possible K1 orientations. These results indicate that the K1 form presents a preferential end-on orientation with NH_3^+ toward the surface.

For K2, the final structures of the three orientations (not shown) are very close to the starting structure. For this form, the **b** orientation has the strongest interaction with the surface, but in general the orientational effects are very weak.

Finally, for K3 in the **a** and **c** starting configurations (see Methods section), the original orientations are kept until the end of the simulations, and for the starting orientations **b**, a final bent orientation is found, similar to the K1b orientation. The total interaction energy between the solvated amino acid molecule and solvated surface is much higher for K3 forms than for the K1 and K2 forms (i.e., yielding lower values of ΔH_i, the lowest being the one for the K3b structure). For all of these K3 structures, the main finding is that α-NH_3^+ tends toward the surface and COO^- points away from the surface.

From these simulations, we can further deduce that the L-lysine−substrate interaction is mainly driven by the electrostatic forces between the charged group NH_3^+ and the silanol groups of the surface, with a relevant H-bond contribution, as revealed by distances, angles,[32] and bond orders (about 0.04[33]) between the hydrogens of the amino group and the oxygen of silanol groups (Table 7).

Furthermore, in the K1b configuration there is an additive contribution due to the attractive interaction between the negative oxygen and positive silicon; this is due to the bending of the molecule, which brings the carboxylate group to point toward the surface. Indeed, the weak bond order between $O_{(carboxylate)}-Si_{(silanol)}$ can be explained in terms of a partial charge transfer from the occupied oxygen orbitals to the unoccupied silicon orbital.

TABLE 7: H-Bond Distances and Relative Angles between the L-Lysine Group and Silanol Groups

	distances (Å) N−H···O−Si	angle (deg) N···H···O
c-K1a	1.93	138.7
c-K1b	2.08	117.3
c-K1c	2.06	138.5
c-K2a	2.09	153.3
c-K2b	2.19	151.1
c-K2c	1.96	167.5
c-K3a	2.35	153.0
c-K3b	2.05	155.6
c-K3c	1.80	154.8

TABLE 8: Relative Average Values of Energy (Potential ΔE_p and Intermolecular ΔE_i) with Respect to the Energy Value of a Form for the Last 40 ps of MD Simulations

	ΔE_p	ΔE_i
s-K1a	0	0
s-K1b	210.9	304
s-K1c	206.1	153.7
s-K2a	80.3	235.5
s-K2b	0	0
s-K2c	116.4	195.6
s-K3a	0	0
s-K3b	27.8	129.8
s-K3c	111.8	−15.5

The L-lysine−surface interaction was studied by analyzing the MD simulations in terms of potential and intermolecular energies, time evolution distances of functional groups from the surface, dihedral angles, and radial distribution functions of water around the amino acid molecule.

In Table 8, we reported the average values of the potential (ΔE_p) and intermolecular (ΔE_i) energies relative to the lowest-energy orientation for the K1−K3 forms.

The time evolution of the distances (not reported here) of functional groups from the surface (indicate by αN and ϵN positions) indicates that, within the statistical fluctuations, K1, K2, and K3 in all orientations remain at a fixed distance from the surface (i.e., in the range of the simulation time (100 ps), there is no dynamical exchange of the L-lysine molecules between the bulk solution and the solid surface).

In particular, for the K1 form the **a** orientation, which keeps a fixed distance of ~1.5 Å from ϵ-NH_3^+ to the surface, is the most stable one. Moreover, as shown in Figure 6, representing the fluctuation of the two nitrogen atoms over the slab plane, the ϵN atom is more localized with the respect to αN because of the "anchoring" effect of ϵ-NH_3^+ to the silanol surface.

At variance with this, in the **b** orientation, where the molecule is kept at a greater distance from the surface, αN is about 4.5 Å from the surface with respect to the other two orientations K1a and K1c. For K1c, it can be seen that the side-on orientation changes after a few time steps, with the approach to the surface of the ϵ-NH_3^+ group (Figure 7a), because of the optimization of the interaction with SiO^-, whereas the COO^- group is displaced away from the surface (Figure 7b). After reaching this condition, the ϵ-NH_3^+ distance from the surface maintains a constant value for the remainder of the simulation period. The analysis of the time evolution of the dihedral angles shows that only in the **c** orientation does the form K1 present different

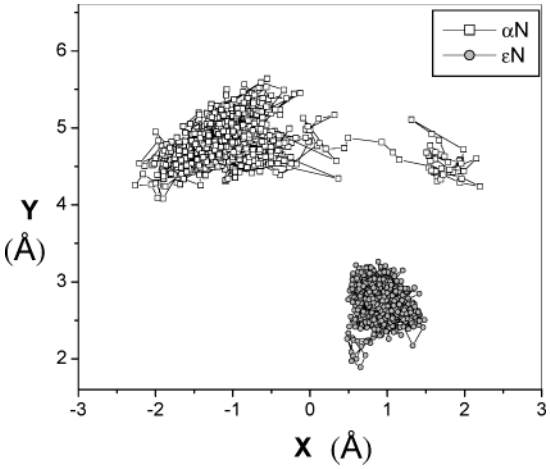

Figure 6. *XY* coordinates of nitrogen atoms of the ϵ-NH_3^+ group (grey circles, ϵN) and of the α-NH_2 group (open squares, αN) in an MD simulation of K1 form an end-on orientation with the ammonium group poiting toward the surface (K1a).

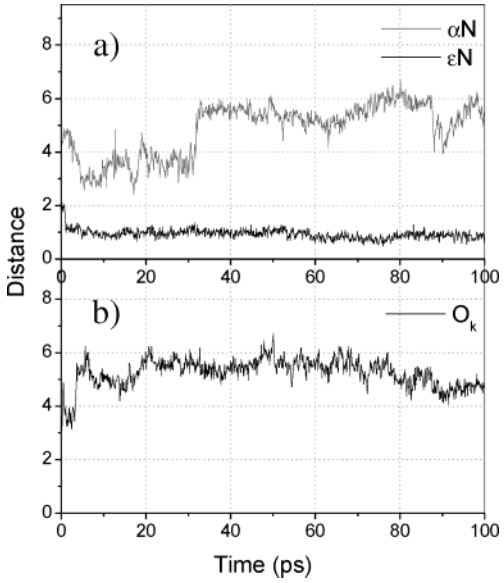

Figure 7. Distances (Å) from the surfaces of functional groups: (a) ϵ-NH_3^+ (grey line, ϵN) and α-NH_2 (black line, αN); (b) oxygen of the carboxylate group (O_k) for the K1 form in a side-on orientation (K1c).

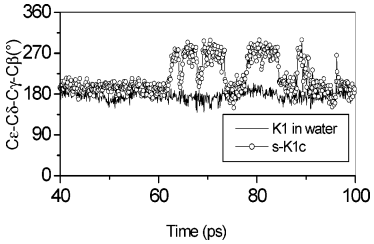

Figure 8. Time trajectories of the dihedral angle $C_\epsilon-C_\delta-C_\gamma-C_\beta$ (deg) in the K1 form along MD simulations with (open circles) and without (black line) the substrate.

behavior with respect to the simulation including water molecules. In particular, in Figure 8 the time evolution of $C_\epsilon-C_\delta-C_\gamma-C_\beta$ indicates that the backbone of the amino acid molecule is forced to make several transitions while approaching the **a** orientation.

Hence, the analysis of the trajectories of the K1 form shows that the preferred orientation is the end-on with ϵ-NH_3^+ pointing toward the surface, whereas for K2 the preferred orientation is **b** (i.e., the end-on configuration with α-NH_3^+ pointing toward

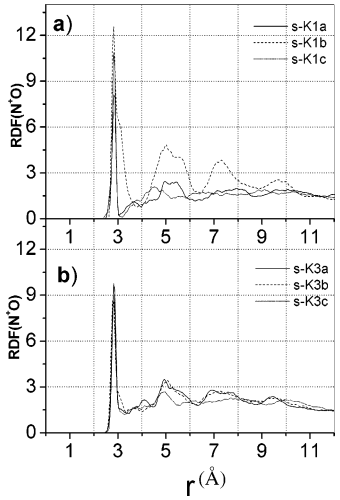

Figure 9. Radial distribution functions of water oxygen around the nitrogen of ammonium group atoms (N^+) of the (a) K1 and (b) K3 forms in MD simulations with the substrate in the tree orientations.

the surface). As to the positively charged form K3, we may observe that ΔE_i (Table 8) and the calculated average distances of αN and ϵN indicate a side-on orientation, supporting the picture of a stronger interaction of this configuration with the surface. In fact, for the K3a form these distances fluctuate around 7.0 and 2.0 Å for αN and ϵN, respectively, whereas these distances are 2.0 and 5.5 Å for K3b and 1.5 and 3.0 Å for K3c, respectively.

The hydration properties for the different configurations were evaluated by analyzing the related radial distribution functions (RDF). In Figure 9, the RDFs of N^+-O(water) are reported, as characteristic examples, for K1 (Figure 9a) and K3 (Figure 9b) forms. This Figure shows clearly the relevant effect of the substrate on the hydration of L-lysine. In particular, the intensity of the first hydration shell for the K1 forms is 2 times greater than the corresponding one without the substrate, the effect being due to the hydrophilic nature of the employed substrate that involves an increased density of the water layer in proximity to the surface.

However, the K1a and K1c forms exhibit a different structure for the outer hydration shells with respect to the K1b form because in this last case a defined structure of the outer hydration shells is maintained, whereas it is almost destroyed in the case of the K1a and K1c forms, where the L-lysine is directly attached to the surface.

However, for K3 forms the RDF profiles show very similar behavior for all of the orientations. In fact, in all cases the first hydration shell is ordered, as indicated from the high intensity of the related RDF feature, whereas the order is lost for the outer shells.

Finally, the RDF structure for the K2 forms does not show any particular differences with respect to L-lysine in solution, confirming that there is a very weak interaction with the surface.

The above-described effect on the RDF structure can be viewed as being due to the disordering action of the approaching molecules to the surface, inducing the perturbation of the outer hydration shells on the surface in absence of L-lysine.

Last but not least, to evaluate the change in the water structure in proximity to the silanol sites, the RDFs of oxygen atoms of water around the oxygen atoms of silanol groups on the surface are analyzed. Accordingly, the RDF structures of water oxygens around silanol oxygens in the presence and absence of L-lysine are reported in Figure 10a. In particular, the RDFs obtained with and without the amino acid molecule were compared for

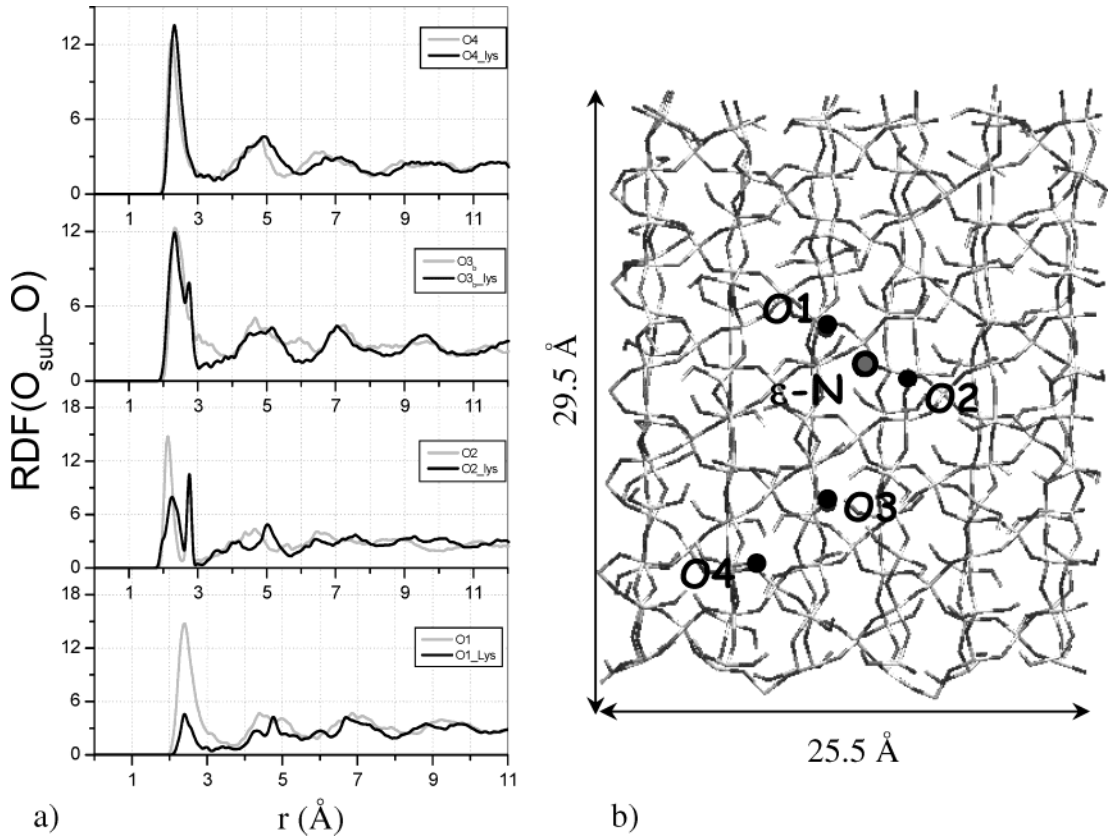

Figure 10. (a) RDF of water oxygen around the oxygen of the surface silanol group (RDF(O_O) with (black line) and without (grey line) the L-lysine molecule. (b) The RDF (O_O) is calculated on the basis of the placement of the oxygen atoms. The silanol oxygen atoms on the surface are indicated by black dots, and the ϵ-N is indicated by a gray dot. O1 and O2 indicate the silanol oxygen that is about 2−3 Å from ϵ-NH_3^+ of K1a, O3 at ∼7 Å, and O4 at ∼11 Å.

O1 and O2 silanol oxygens at about 2−3 Å from the ϵ-NH_3^+ of K1a, for O3 at ∼7 Å, and for O4 at ∼11 Å (Figure 10b). Relevant effects can be seen only for the cases of O1 and O2, which are closer to L-lysine. O3 and O4 show the typical situation of an unperturbed hydration structure, being too far from the region perturbed by the L-lysine presence. The very same effect is seen for the K3c RDF (not shown here).

4. Summary and Conclusions

A molecular modeling technique was applied to investigate L-lysine on a hydroxylated quartz surface. Theoretical investigations were performed at quantum and classical levels to study the static properties of the adsorbing molecules, and molecular dynamics techniques were used to address the time evolution of the adsorption process. As expected, solvation effects play a key role in determining the nature and the strength of the molecule−surface interaction, which in turn strongly affect both the static and dynamic properties. As a matter of fact, it appears clearly that a realistic calculation needs to include explicitly water molecules and the related solvation shell structure in the calculations, as far as it is not possible to employ the COSMO technique for surface-related systems because of the unphysical situation that it would require involving the presence of solvent molecules within the solid.

As to the static properties, the preliminary study performed on L-lysine molecule in "bulk" water solution allowed to understand the relative importance of the various amino acid forms at the isoelectric pH. In particular, it resulted that the most stable form is the zwitterionic K1 structure, with the ammonium group located at the end of the side chain.

As a successive step, we have focused our attention on the amino acid orientation effects induced by the presence of a well-defined hydroxylated quartz surface. Accordingly, semiempirical quantum mechanics calculations, used to obtain qualitative and quantitative estimation of molecule/surface interaction, showed that the nature of this interaction is mainly electrostatic with some H-bond contribution. Furthermore, the analysis of the optimized final structures indicates that the preferred one is the zwitterionic form K1 in the end-on orientation with ϵN pointing toward the surface. As to the addressed problem, this represents the main result of the present paper.

As to the dynamic properties, not only did the MD calculations confirm the preference for the above-described orientation but also, more importantly, the structure of water layers at the interface with the substrate, with and without the amino acid molecule, was obtained. The change in the water structure in the presence of the adsorbed amino acid, consisting of the breaking down of the more external water shells with respect to the substrate, was observed because of the reciprocal perturbation of the molecule and surface solvation shells.

Furthermore, an additional perturbation effect could be identified in connection with the adsorption properties of the aliphatic chain of L-lysine, which enhances the disordering effect in the case of the side-on orientation of the amino acid molecule, thus providing a further driving force for the prevailing end-on orientation. In particular, the calculations demonstrate that the water gives an indirect cooperative contribution to L-lysine−surface interactions, decreasing the size of the solvation shell around the charged groups NH_3^+ and SiO^-. Furthermore, in our opinion, a more important cooperative effect of the solvent

on the L-lysine−surface interaction could occur in the case of two or more L-lysine molecules closely adsorbed on the silanol-rich surfaces here investigated.

Further work is currently in progress in the study of this more complex system.

Acknowledgment. We acknowledge financial support from PF "MSTA II" (CNR, Rome) and PRIN 2002 (MIUR, Rome).

References and Notes

(1) Horbett, T. A. Protein Adsorption on Biomaterials. In *Biomaterials: Interfacial Phenomena and Applications*; Copper, S.L., Peppas, N.A., Eds; American Chemical Society: Washington, DC, 1982; p 233.
(2) Lee J. H.; Tonglei L. *Water in Biomaterials Surface Science*; Morra, M., Ed.; Wiley & Sons: New York, 2001; pp 127−146.
(3) Csàszàr, A. G. *J. Am. Chem. Soc.* **1992**, *114*, 9569.
(4) Tuñón, I.; Silla, E.; Ruiz-López, M. F. *Chem. Phys. Lett.* **2000**, 433.
(5) Csàszàr, A. G. *J. Phys. Chem.* **1996**, *100*, 3541.
(6) Shirazian, S.; Gronert, S. *J. Mol. Struct.: THEOCHEM* **1997**, *397*, 107.
(7) Tortonda, F. R.; Silla, E.; Tuñón, I.; Rinaldi, D.; Ruiz-López, M. F. *Theor. Chem. Acc.* **2000**, *104*, 89.
(8) Pertsemlidis, A.; Safena, A. M.; Soper, A. K.; Head-Gordon, T.; Glaeser, R. M. *Proc. Natl. Acad. Sci. U.S.A.* **1996**, *93*, 10769.
(9) *Silicon and Siliceous Structures in Biological Systems*; Simpson, T. L., Volcani, B. E., Eds.; Springer-Verlag: New York, 1981.
(10) Li, H.; de Bruyn, P. *Surf. Sci.* **1986**, *5*, 203.
(11) House, W. A.; Orr, D. R. *J. Chem. Soc., Faraday Trans.* **1992**, *88*, 233.
(12) Stumm W. *Colloids Surf., A* **1997**, *120*, 143.
(13) McFarlan, A. J.; Morrow, B. A. *J. Phys. Chem.* **1991**, *95*, 5388.
(14) Koudriachova, M. V.; Beckers, J. V. L.; de Leeuw, S. W. *Comput. Mater. Sci.* **2001**, *20*, 381.
(15) Xiao, Y.; Lasaga, A. C. *Geochim. Cosmochim. Acta* **1996**, *60*, 2283.
(16) Rustad, J. R.; Wasserman, E.; Felmy, A. R.; Wilke, C. *J. Colloid Interface Sci.* **1998**, 198.
(17) Sverjensky, D. A.; Sahai, N. *Geochim. Cosmochim. Acta* **1996**, 60, 20, 3773.
(18) West, J. K.; Latour, R. Jr.; Hench L. L. *J. Biomed. Mater. Res.* **1997**, *37*, 585.
(19) West, J. K., Hench L. L. *J. Biomed. Mater. Res.* **1994**, *28*, 625.
(20) McClung, W. G.; Clapper, D. L.; Hu, S.-P.; Brash, J. L. *Biomaterials* **2001**, *22*, 1919.
(21) Tayyab, S.; Haq, S. K.; Sabeeha; Aziz M. A.; Khan M. M.; Muzammil S. *Int. J. Bio. Macromol.* **1999**, *26*, 173.
(22) Remelli, M.; Conato, C.; Agarossi, A.; Pulitori, F.; Młynarz, P.; Kozłowski, H. *Polyhedron* **2000**, *19*, 2409.
(23) Stewart J. J. P. *MOPAC2000 Manual*; Fujitsu Limited: Tokyo, 1999.
(24) Klamt, A.; Shuurmann, G. *J. Chem. Soc., Perkin Trans* **1993**, *2*, 779.
(25) Ponder W. J. *TINKER, Software Tools for Molecular Design*, version 3.6.
(26) (a) Sorensen, J. B.; Lewin, a. H.; Bowen, J. P. *J. Mol. Struct.: THEOCHEM* **2003**, *623*, 145. (b) Allinger, N. L.; Yuh, Y. H.; Lii, J.-H. *J. Am. Chem. Soc.* **1989**, *111*, 8551. (c) Lii, J.-H.; Allinger, N. L. *J. Comput. Chem.* **1998**, *19*, 1001. (d) Sorensen, J. B.; Lewin, a. H.; Bowen, J. P. *J. Phys. Org. Chem.* **2001**, *66*, 4105.
(27) Koetzle, T. F.; Lehmann, M. S.; Verbist, J. J.; Hamilton, W. C. *Acta Crystallogr., Sect. B* **1972**, *28*, 3207.
(28) Beest, B. W. H.; Kramer, G. J.; Santen, R. A. *Phys. Rev. Lett.* **1990**, *16*, 64.
(29) McNamee, C.; Matsumoto M.; Hartley, P. G.; Nakamara, M. *Colloids Surf., A* **2001**, *193*, 1−3, 175.
(30) Rustad, J. R.; Hay, B. P. *Geochim. Cosmochim. Acta* **1995**, *59*, 7, 1251.
(31) Unpublished results.
(32) Adalsteinsson, H.; Maulitz, A. H.; Bruice T. C. *J. Am. Chem. Soc.* **1996**, *118*, 7689.
(33) Buemi, G. *J. Mol. Struct.: THEOCHEM* **2000**, *499*, 21.